

A Generative Shape Compositional Framework: Towards Representative Populations of Virtual Heart Chimaeras

Haoran Dou, Seppo Virtanen, Nishant Ravikumar*, Alejandro F. Frangi*

Abstract—Generating virtual populations of anatomy that capture sufficient variability while remaining plausible is essential for conducting *in-silico* trials of medical devices. However, not all anatomical shapes of interest are always available for each individual in a population. Imaging examinations and modalities employed and available can vary across individuals. Different imaging modalities may have different fields of view, be sensitive to signals from different tissues/organs, or both. Hence, missing/partially-overlapping anatomical information is often available across individuals in a population. We introduce a generative shape model for complex anatomical structures, learnable from datasets of unpaired datasets, i.e. where each substructure in the complex comes from datasets that have missing or partially overlapping substructures from disjoint subjects of the same population. The proposed generative model can synthesise complete whole-complex shape assemblies coined *virtual chimaeras*, as opposed to natural human chimaeras. We applied this framework to build *virtual chimaeras* from databases of whole-heart shape assemblies that each contribute samples for heart substructures. Specifically, we propose a graph neural network-based generative shape compositional framework which comprises two components - a part-aware generative shape model which captures the variability in shape observed for each structure of interest in the training population; and a spatial composition network which assembles/composes the structures synthesised by the former into multi-part shape assemblies (viz. *virtual chimaeras*). We also propose a novel self-supervised learning scheme that enables the spatial composition network to be trained with partially overlapping data and weak labels. We trained and validated our approach using shapes of cardiac structures derived from cardiac magnetic resonance images available in the UK Biobank. When trained with *complete* and *partially overlapping* data, our approach significantly outperforms a PCA-based shape model (trained with *complete* data) in terms of generalisability and specificity. This demonstrates the superiority of the proposed approach as the synthesised cardiac virtual populations are more plausible and capture a greater degree of variability in shape than those generated by the PCA-based shape model.

Index Terms—*In-silico* trials, virtual populations, graph neural network, generative model.

I. INTRODUCTION

IN-*silico* trials (ISTs) proffer a paradigm shift for medical device innovation and the regulatory approval process

Haoran Dou, Seppo Virtanen, Nishant Ravikumar, and Alejandro F. Frangi are with the Center for Computational Imaging & Simulation Technologies in Biomedicine (CISTIB). Haoran Dou, Nishant Ravikumar and Alejandro F. Frangi are part of the School of Computing, Seppo Virtanen is part of the School of Mathematics at University of Leeds, Leeds, LS2 9JT, UK (e-mail: h.dou1@leeds.ac.uk).

* Nishant Ravikumar and Alejandro F. Frangi are joint last authors.

which underpins the route to commercialisation of devices and their adoption in routine patient care. Traditionally, gathering scientific evidence for regulatory approval of novel devices and drugs required in-vitro and in-vivo assessment of safety and efficacy. This practice, however, poses a methodological and economic burden on medical products that hinder innovation and delay/impede patient benefit. In response, regulatory agencies are increasingly embracing complementary sources of evidence that refine, replace and reduce the need for animal and human testing [1]. ISTs use computational modelling and simulation to evaluate the safety and efficacy of medical devices virtually, in digital twin or virtual patient (VPs) populations, and provide digital (or *in-silico*) as opposed to real-world evidence supporting regulatory approval of devices. ISTs thus have the potential to explore device performance in a wider range of patient characteristics than feasible to recruit for in a real clinical trial. They could help refine, reduce, and partially replace *in vivo* clinical trials.

Correspondingly, ISTs require generation of digital twin or virtual patient populations that capture sufficient anatomical and physiological variability, representative of target patient populations, to enable meaningful *in-silico* assessment of device performance. We focus on the challenge of generating representative populations of anatomy, specifically, cardiovascular anatomy, in this study. We also define digital twins as distinct from virtual patients in the following way - digital twins are considered to be patient-specific replicas of anatomical structures, generated by segmenting medical images (e.g. magnetic resonance (MR) or computed tomography (CT) images) of patients and representing the shape of anatomical structures of interest in some parametric form (e.g. triangular surface meshes). Virtual patients on the other hand, are considered to be parametric representations of anatomical structures sampled from a generative model (e.g. probabilistic PCA, variational autoencoder (VAE)), where the latter was learned from a population of digital twins. On the other hand, virtual patients represent no specific real subject/patient's anatomy, but are instances generated from a trained model. We introduce *virtual chimaeras* (VCs), as opposed to natural human chimaeras [2], as distinct entities from VPs in the following way - a VC is a parametric representation of anatomical structures sampled from a generative model trained using *partially overlapping* data, i.e. where all anatomical structures of interest are not available for all individuals in the training population. This is distinct from VPs as we define them as instances of statistical/generative models that require *complete overlap* in

the training data. I.e. where all anatomical structures of interest are available for all individuals in the training population (e.g. PCA). Henceforth, we will refer to these scenarios that lead to VCs and VPs as learning statistical/generative shape models with '*partial overlap*' or '*complete overlap*' in training data for brevity.

A. Virtual Population Modeling

Virtual populations of anatomical shapes (typically represented as computational meshes) are essential for conducting ISTs of medical devices. However, building rich/descriptive generative shape models of multi-part anatomical structures is challenging. Most techniques require large volumes of training data comprising the same semantic parts/shapes in each training sample. This would require expensive and laborious annotation of medical imaging data to ensure anatomical shapes of interest can be accurately extracted from each subject/sample, which is prohibitive. Relying on complete annotations precludes using of existing public databases where annotations for a few anatomical structures of interest may already be available. Additionally, specific anatomical structures may only be visible/easy to delineate in specific image modalities that are less prevalent. For instance, cine-MR images do not capture the 3D structure of atria or the aorta within the field of view. However, large-scale databases such as the UK Biobank are available (comprising >40k subjects' images). In contrast, computed tomography angiography (CTA) captures fine-details of all four cardiac chambers and the associated great vessels (e.g. aorta and pulmonary artery) in 3D owing to its high spatial resolution. Still, it brings the added risk of patient exposure to radiation. Consequently, the scale of CTA data publicly available is usually much smaller than cine-MRI.

While a few studies in the computer vision domain [3], [4] have investigated learning multi-part generative shape models using disparate data sets with non-/partially-overlapping parts (i.e. where individual parts from different data sets are leveraged to learn a model that synthesises multi-part shape assemblies), this remains unexplored within the medical imaging domain to the best of our knowledge. Given the deluge of annotated medical imaging data (characterising anatomical structures of interest) that have been curated in recent years, which is likely to increase in coming years, there is a need in the medical image computing community to develop techniques that facilitate the estimation of multi-part generative shape models, by using anatomical structures that may be available in multiple disparate populations/databases and image modalities.

B. Relevant Literature

This study focuses on generating virtual populations of cardiovascular anatomy, represented as triangular surface meshes. While several previous studies have proposed image-based generative models that capture anatomical variability across a population, we restrict our discussion of relevant literature to previous work on statistical/generative shape modelling. Similarly, early work on statistical shape models (SSMs)

was motivated by the need for model-constrained image segmentation approaches to preserve the topology of segmented anatomical structures, by using SSMs as a shape prior. A detailed review of these methods however, is beyond the scope of this study and we refer the reader to the review by Heimann *et al.* [5] for more information on the topic.

PCA-based statistical shape modelling is the most common approach to building virtual populations of anatomical shapes thus far. SSMs learned using PCA were popularised by [6] and have been used extensively for generating virtual populations of anatomy [7], [8], quantitative shape analysis for computer-aided-diagnosis [9] and in model-based segmentation [10] approaches. SSMs have also been used extensively in the cardiovascular domain to explore associations between cardiac morphology and function [11], [12], for cardiac image segmentation [13]–[15], and to characterise shape variability across healthy [16] and pathological populations [17]. Inspired by [18], the first study to construct a multi-part SSM of the heart, several subsequent studies [19]–[21] have employed PCA and its variants to build 4D (3D+time) statistical models that can capture inter- and intra-subject spatio-temporal variability in cardiac shape, simultaneously. For example, Hoogendoorn *et al.* [22] decoupled the inter-subject shape and intra-subject temporal (dynamic) variations through a bilinear model, enabling extrapolation of cardiac phase from the SSM even in the absence of individual measurements.

PCA-based SSMs generate virtual shape populations by sampling from the shape-space spanned by an orthogonal set of basis vectors, i.e. the eigenvectors (or principal components) of the covariance matrix of the population of shapes used to build the model. Both point set and mesh-based representations of anatomical structures have been used to build SSMs in this way. However, a pre-requisite for PCA-based SSMs is point-wise correspondence across the population of training shapes (typically achieved via co-registration of shapes before SSM construction) and *complete overlap* across all samples in the training population. In other words, standard PCA-based SSMs cannot handle missing structures or effectively use training samples with *partial overlap* in anatomical structures. Recent advances in deep learning have demonstrated that deep neural networks can be formulated as powerful generative models for both images and geometric (e.g. point clouds, meshes/graphs) data, due to their ability to learn rich hierarchical representations of data [23]. A few studies [24]–[28] have adopted these approaches for generating virtual populations of anatomy. For example, Beetz *et al.* [24] used a variational auto-encoder (VAE) [29] to learn latent representations of cardiac biventricular anatomy represented as point clouds. They equipped the network with additional inputs of population-specific characteristics to enable conditional synthesis of biventricular anatomies. Romero *et al.* [26] explored the generation efficiency of the generative adversarial network (GAN) [30], trained on binary masks of aortas. Danu *et al.* [28] employed a deep generative model to generate voxelised vessel surfaces and ensure compatibility between the unstructured representation (points/polygons) of vessel surfaces, and the structured domain required for the application of convolutional neural networks. Bonazzola *et al.* [27] utilised

a graph convolutional VAE to learn latent representations of image-derived 3D left ventricular meshes, and used the learned representations as surrogates for cardiac phenotypes in genome-wide association studies.

The success of compositional learning in computer vision shows an exceptional possibility to obtain a diversity shape model by merging the shape variability of multiply objects. Although effective, all aforementioned methods were designed for single-part anatomies [26], or require *complete overlap* across all training samples in terms of the presence/absence of anatomical structures of interest in multi-part shape assemblies [24]. Such techniques therefore, fail to maximise the value of multiple disparate datasets with *partially overlapping* anatomical structures, limiting the variability that can be synthesised in multi-part shape assemblies (as the training population is limited to samples exhibiting *complete overlap*). Recent advances in shape *compositional* learning [3], [31], [32] within the computer vision domain, look to address these limitations by leveraging complementary information available in disparate data sets to build rich generative models of multi-part shape assemblies. For instance, Li *et al.* [31] proposed to learn the 3D shape synthesis through a two-stage framework including part generation and assembly. GIRAFFE [3] modeled the scenes through the compositional neural feature fields.

C. Contributions

This study proposes a generative shape *compositional* learning framework based on graph-convolutional neural net to generate virtual cohorts of cardiovascular structures (represented as surfaces meshes/undirected graphs). We referred to the synthesised constructs as *virtual chimaera* cohorts to enable disparate datasets with partially-overlapping anatomical structures to be leveraged for learning a generative model of multi-part shape assemblies. Although the proposed generative framework is demonstrated here on cardiovascular structures, it is generic by design and applicable to other multi-structure/organ ensembles. The key contributions of this study are:

- 1) This is the first study to tackle the problem of combining data from different subjects with *partially-overlapping* anatomical structures, in a generative shape modelling framework to synthesise multi-part shape assemblies representative of native anatomy. We refer to instances synthesised by the proposed approach as *virtual chimaeras*.
- 2) While generative shape compositional learning was previously proposed within the computer vision domain, this is the first study to propose an approach for synthesising multi-part assemblies of anatomical structures.
- 3) Existing generative shape compositional learning approaches have used composition networks that predict rigid or affine transformations to compose the individual parts synthesised into multi-part assemblies. We extend these approaches by including a non-rigid registration component in our composition network to reduce topological errors such as gaps or mesh intersections between

individual parts (anatomical structures) of the shape assembly.

- 4) Existing approaches to generative shape compositional learning have relied on *strong supervision* for training the composition network, i.e. where either the ground truth transformations are known *a priori*, or where the ground truth complete multi-part shape assembly is available for each training sample. This precludes the use of partially-overlapping data (the main motivation of this study) for this purpose. We address this limitation by proposing a novel self-supervised approach for training the composition network.

Building generative models of multi-part shape assemblies (such as the cardiovascular structures considered in this study, namely, four cardiac chambers and the root of the aortic vessel) is challenging due to the distinct variability in shape of each part, often the varying topology between the individual parts, and typically, the need for a suitable training set where all parts/structures of the shape assembly of interest are available for all samples (which precludes the combination of multiple datasets with partially-overlapping anatomical structures). It is therefore desirable to formulate a generative framework that can effectively capture the variability in shape of each part in an assembly, can accommodate varying topology across parts and finally, is not dependent on the availability of all parts of the shape assembly, across all samples in the training set. To facilitate this we explore two different generative approaches for learning part-aware latent representations of five cardiovascular structures (i.e. four cardiac chambers and the aortic root) and explore them within the proposed compositional framework. Henceforth, these two approaches are referred to as the *independent generator* and *dependent generator*. The *independent generator* comprises five independent graph-convolutional variational autoencoders (gcVAEs), corresponding to the five cardiovascular structures of interest. The *dependent generator* is a novel graph-convolutional multi-channel variational autoencoder (mcVAE). These are regarded as minor contributions of the study in addition to the core contributions (1-4) listed above as - (i) convolutional mesh autoencoders (CoMA) [33] and gcVAEs [34] were proposed previously for different applications on 3D face reconstruction and deformable shape completion, respectively; and (ii) the mcVAE was also proposed previously for learning shared latent representations of multi-modal images [35]. Our contributions in this regard are thus restricted to the use of these approaches within a novel shape compositional learning framework, and the formulation of a graph-convolutional variant of the mcVAE. Finally, we also propose new metrics for evaluating the quality of synthesised virtual cardiac cohorts, in terms of the overall variability in shape captured across the synthesised *virtual chimaeras*, their anatomical plausibility, and their clinical relevance evaluated as ratios of standard cardiac volumetric indices, referred to as ‘clinical acceptance criteria’.

II. METHODOLOGY

The proposed deep shape compositional framework, for synthesising cardiac virtual populations, is described by the

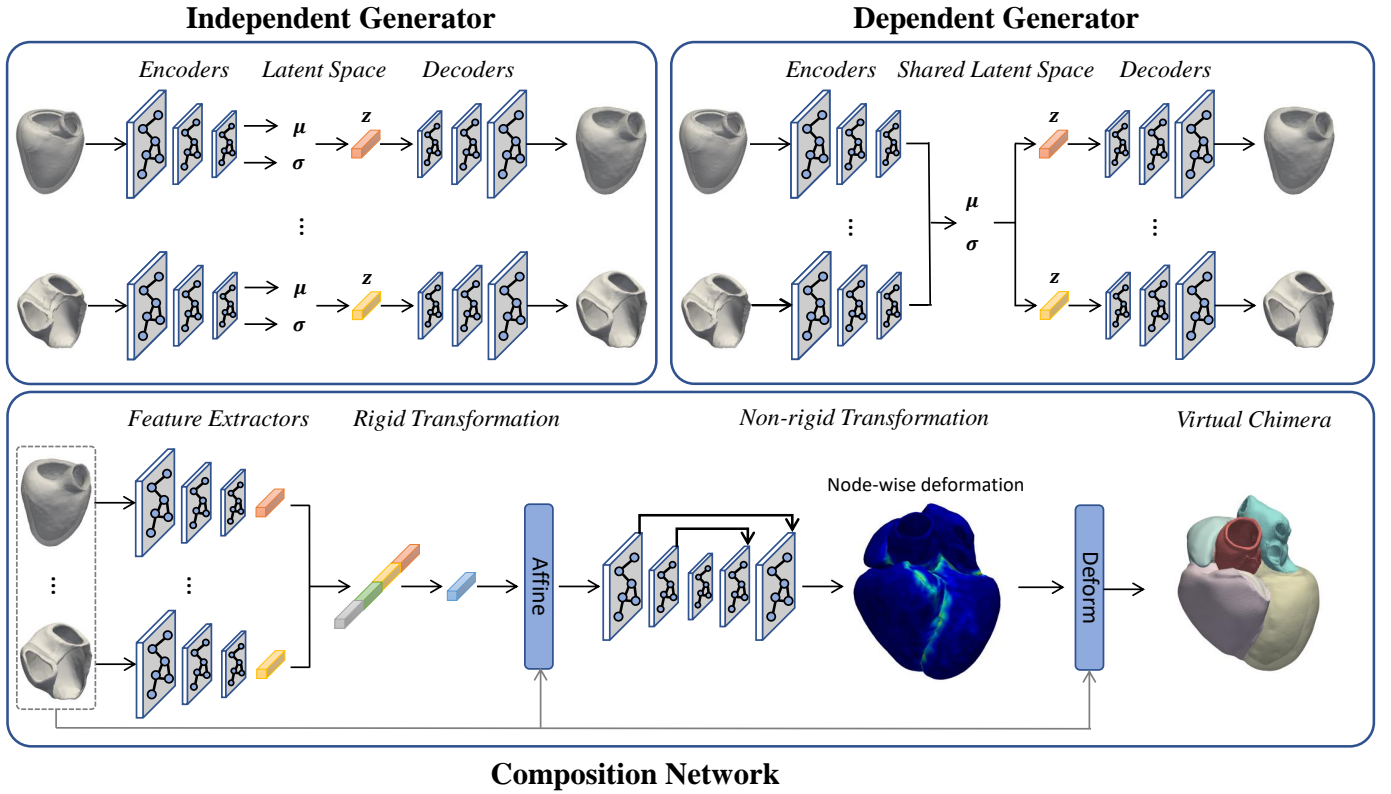


Fig. 1. Schematic illustration of our proposed shape compositional framework, which consists of a part-aware generator to learn the shape representations of each part and a composition network to perform the rigid and non-rigid transformation to compose the synthetic parts to the whole heart shape.

schematic shown in Figure. 1. It comprises two modules, namely, a *part-aware generative model* and a *composition network*. The part-aware generative model can be formulated in several ways, using traditional statistical/machine learning approaches (e.g. PCA, probabilistic PCA, etc.) or recent geometric deep learning approaches (e.g. gcVAEs). In this study, we explore two generative schemes based on graph-convolutional neural networks: the *independent generator* and the *dependent generator*. The independent generator learns latent representations of each part individually, where each sub-generator is a gcVAE specific to its part. This provides flexibility in the overall generative framework, as each part-wise gcVAE is trained independently, enabling *partially overlapping* patient data to train each gcVAE. Additionally, as each gcVAE explicitly models the part-wise variability in shape observed across the training population(s), we argue that their combination within the proposed shape composition framework can synthesise virtual cardiac cohorts that capture a greater degree of variability in shape, than afforded by using a single gcVAE (or similar model, e.g. PCA) to model all parts in the shape assembly jointly.

Conversely, the dependent generator learns a shared latent representation across all parts in a shape assembly (i.e. all four cardiac chambers and the aortic root in this study) using a graph-convolutional mcVAE [35] network. The dependent generator models the joint likelihood of the observed data, i.e. of all parts in the shape assembly, as a product of the conditional likelihoods of each part, conditioned on the other observed parts, the shared latent variables, and the model

parameters. Estimating shared latent variables in this manner promotes anatomical plausibility in the shapes synthesised using the learned latent representation as the latter captures the co-variation observed across multiple parts in the training population(s). As the dependent generator learns a shared latent representation of all parts in a shape assembly, the model by design enables conditional synthesis of one or multiple parts, given one or more other parts as inputs. Correspondingly, the dependent generator can also be trained using *partially overlapping* patient data. Not all parts in a shape assembly of interest are available in all samples considered in the training population(s). We explore the independent and dependent generator within the proposed shape compositional framework to compare their relative merits. For example, an approach designed to enhance the overall variability in anatomical shape captured (as in the former), versus one designed to promote anatomical plausibility (as in the latter), in the synthesised cardiac *virtual chimaera* cohorts.

Cardiovascular structures synthesised using the part-aware generator (based on either the independent or dependent generator) are initially not spatially composed. They hence do not represent anatomically plausible whole heart shapes. A *composition network* must facilitate the latter. The composition network comprises a deep graph-convolutional neural network that first estimates 3D affine transformations to spatially organise each synthesised part/cardiovascular structure into a valid shape assembly. I.e. the synthesised parts are transformed such that their relative positions and orientations to each other are consistent with native anatomy. Subsequently, the

composition network refines the shape assembly by estimating a non-rigid transformation that locally deforms the nodes at interfaces between adjacent parts in the assembly. This non-rigid transformation step is necessary as affine transformations alone could result in gaps, intersections between adjacent parts in a shape assembly, which is reduced through the former, or both. The output of the composition network is a composed whole heart mesh/shape assembly, representing a cardiac *virtual chimaera* instance (as illustrated in Fig. 1).

A. Part-Aware Generative Model

As discussed, the part-aware generative model enables semantic part-wise synthesis of the cardiovascular structures of interest, namely, four cardiac chambers and the aortic root, using either the independent or dependent generator. We select graph convolution operations based on truncated Chebyshev polynomials [36], and adopt mesh downsampling and upsampling operations as in CoMA [33], to construct the encoder-decoder networks for both the independent and dependent generator. As shown in Fig. 1, each encoder-decoder network pair in the independent and dependent generator takes a triangular surface mesh of a part/cardiovascular structure as input and outputs the reconstructed surface mesh. Each mesh is represented by a list of 3D spatial coordinates of its vertices and an adjacency matrix defining vertex connectivity (i.e. edges of mesh triangles). Mesh downsampling and upsampling operations in the network help capture both global and local shape context and are defined over a multi-resolution mesh hierarchy based on quadric edge collapses [37]. The hierarchy is divided into five resolution levels. Features are learned at each resolution level using a graph convolution block with two constituent graph convolution layers. In the encoder, the number of feature channels within each layer in each of the five blocks is 16, 32, 32, 64 and 64, respectively, with increasing network depth. Similarly, the same number of channels are used in reversed order, for each block in the decoder.

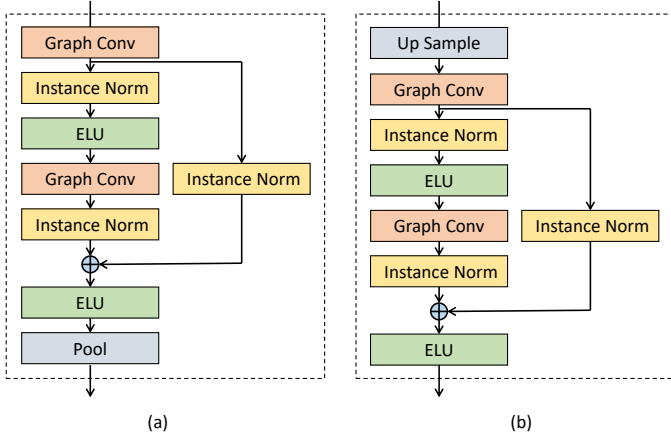


Fig. 2. Schematic illustration of the graph convolution blocks. (a) is the architecture of the residual graph convolution block in encoder and (b) is that in the decoder.

To strengthen the feature exchange efficiency between vertices [38] and mitigate the issue of vanishing gradients when

training the network, we replace the basic graph convolution block used in [33], with a residual block (shown in Fig. 2). Each residual block comprises two graph convolution layers that extract features using the provided inputs to the block, and a residual connection [39] that combines the output of the first and second graph convolution layers through summation. Chebyshev graph convolution operations are used throughout this study due to their strictly localised filters that enables learning of multi-scale hierarchical patterns when combined with mesh pooling operations, and low computational complexity. Each graph convolution layer is followed with an instance normalisation layer [40] and an exponential linear unit (ELU) [41] for activation. Additionally, an instance normalisation layer is used in the residual branch to ensure similarity in feature statistics relative to the output of the second graph convolution layer in the block.

The part-aware generative model, both in the case of the independent and dependent generator, is trained by optimising a composite loss function that combines three different losses. The independent and dependent generators are Bayesian models based on VAEs. The latent space from which the observed data \mathbf{X} is generated, can be discovered by approximating the posterior distribution of the latent variables using variational inference [29]. This is achieved by optimising the evidence lower bound (ELBO) of the observed data concerning the networks' parameters, which can be formulated as a summation of the expected reconstruction error (i.e. expected negative log-likelihood of the data) and the Kullback-Leibler divergence of the approximate posterior distribution of the latent variables, from their assumed prior (as shown in [29]). Based on this formulation of the ELBO, we construct our composite loss function to include: a reconstruction loss \mathcal{L}_{recon} based on the vertex-wise L_1 -norm computed between the predicted and original mesh vertices; the Kullback-Leibler divergence \mathcal{L}_{KL} between the approximate posterior distribution of the latent variables $q(\mathbf{z}|\mathbf{X})$, and the prior distribution over the latent variables $p(\mathbf{z}) \sim \mathcal{N}(\mathbf{0}, \mathbf{I})$, i.e. a multivariate Gaussian prior with unit variance is used throughout this study for both the independent and dependent generator; and an additional regularisation loss $\mathcal{L}_{regular}$ that penalises outliers and encourages smooth surface reconstructions. The key difference between the independent and dependent generator lies in the formulation of \mathcal{L}_{recon} , i.e. the expected negative log-likelihood of the observed data \mathbf{X} . The composite loss function used to train each part-wise gcVAE in the independent generator, and the graph-convolutional mcVAE in the dependent generator, is given by,

$$\mathcal{L} = \mathcal{L}_{recon} + \omega_0 \mathcal{L}_{KL} + \mathcal{L}_{regular} \quad (1)$$

where, ω_0 denotes the weight of the \mathcal{L}_{KL} loss. The reconstruction loss \mathcal{L}_{recon} for each gcVAE in the independent generator is computed as,

$$\mathcal{L}_{recon} = \|\mathbf{X}_c - \mathbf{X}'_c\|_1 \quad (2)$$

where, \mathbf{X}_c and \mathbf{X}'_c denote the input and reconstructed mesh of part c . As the dependent generator is a graph-convolutional mcVAE which learns a shared latent representation across all $c = \{1 \dots C\}$ parts in a shape assembly, the joint data likelihood

across all parts $\mathbf{X}_{c=1..C} \in \mathbf{X}$ can be expressed as $p(\mathbf{X} \mid \mathbf{z}) = \prod_{c=1}^C p(\mathbf{X}_c \mid \mathbf{z})$ by assuming each part to be conditionally independent from the others (conditioned on \mathbf{z}). Based on this assumption the reconstruction loss \mathcal{L}_{recon} is computed as,

$$\mathcal{L}_{recon} = \sum_{c=1}^C \sum_{c'=1}^C \|\mathbf{X}_c - \mathbf{X}'_{c|c'}\|_1 \quad (3)$$

where, $\mathbf{X}'_{c|c'}$ is the reconstructed mesh of part c conditioned on the shared latent space of all parts $c' = \{1..C\}$. This formulation of the joint data likelihood based on the mcVAE [35] enables reconstruction of a multi-part shape assembly given a single part as input. Additionally, complete multi-part shape assemblies can be sampled from the shared latent space learned.

Finally, $\mathcal{L}_{regular}$ is formulated identically for both the independent and dependent generator and contains two terms: a Laplacian smoothness loss and an edge length loss. The Laplacian loss is used to encourage the neighbouring vertices to move coherently, thus reducing mesh self-intersections and encouraging smoother surface reconstructions [42]. Given vertex \mathbf{v} and neighbouring vertices \mathbf{v}_k , where, $\mathbf{v}_k \in N(\mathbf{v})$, it is defined as:

$$\mathcal{L}_{Laplacian} = \sum_{\mathbf{v}} \left(\mathbf{v} - \sum_{\mathbf{v}_k \in N(\mathbf{v})} \frac{1}{\|N(\mathbf{v})\|} \mathbf{v}_k \right) \quad (4)$$

The edge length loss penalises spurious motion of vertices relative to k neighbouring vertices and is defined as,

$$\mathcal{L}_{edge} = \sum_{\mathbf{v}} \sum_{\mathbf{v}_k \in N(\mathbf{v})} \|\mathbf{v} - \mathbf{v}_k\|_2 \quad (5)$$

Therefore the overall regularisation loss $\mathcal{L}_{regular}$ is defined as the weighted summation of the both losses mentioned above and is given by,

$$\mathcal{L}_{regular} = \omega_1 \mathcal{L}_{Laplacian} + \omega_2 \mathcal{L}_{edge} \quad (6)$$

The weights associated with the terms in the composite loss function (ω_0, ω_1 and ω_2) are hyperparameters that were tuned and set empirically.

B. Spatial Composition Network

Once the part-aware generative model is trained, using either the independent or dependent generator, all parts in the shape assembly can be sampled from the model. Since each part is generated separately, their spatial positions and orientations relative to one another are not consistent with native anatomy. Consequently, synthesised parts when initially assembled may have significant intersections/overlaps with other parts or large gaps with certain parts that they are meant to share boundaries with, as per native anatomy. Thus, learning the spatial relationships between parts in the assembly is imperative to estimate the spatial transformations necessary to compose the individual parts synthesised into a whole heart shape assembly that is consistent with native anatomy. Previous studies on shape composition learning in the computer vision domain [31], [43] have relied on rigid registration

for assembling synthesised individual parts using a dedicated composition network, and have predominantly applied such a generative framework to solid structures such as, chairs, tables, airplanes, etc. However, due to the deformable nature of soft tissue, cardiovascular structures exhibit localised non-linear variations in shape across patient populations. Consequently, rigid/affine transformations alone are insufficient to accommodate such localised shape variations, and to compose the individual parts synthesised into whole heart shape assemblies that are consistent with native anatomy. Therefore, we propose a composition network that estimates the affine and non-rigid transformations sequentially (see Fig.1). The estimated affine and non-rigid transformations in turn, spatially compose the cardiovascular structures synthesised by the part-aware generator into whole heart shape assemblies. Furthermore, we distinguish from previous approaches to shape composition learning [31], [43] that rely on strong supervision to estimate the necessary spatial transformation. Instead, we propose a self-supervised learning scheme, driven by the shared vertices between adjacent structures in the shape assembly (known *a priori*), to estimate the desired affine and non-rigid transformations.

Figure 1 shows our composition network, which takes the generated shapes of each cardiovascular structure (i.e. four cardiac chambers and the aortic root) as input and outputs the composed whole heart shape. Synthesised parts are first passed to the affine registration module of the composition network. This affine registration module comprises part-specific sub-networks utilising the same architecture as each encoder in the independent generator, which are trained simultaneously to extract features from the input shapes. These features are aggregated via concatenation and used to guide the estimation of the desired affine transformations (see Fig.1), denoted $\mathcal{T}_{c=1..C}$, resulting in an initial coarsely composed whole-heart shape. Here, the subscript denotes the c^{th} part in the shape assembly.

The 3D affine transformations estimated comprise eight parameters, including translation ($[T_x, T_y, T_z]$), scaling (S), and rotation ($[Q_1, Q_2, Q_3, Q_4]$ parameterised using quaternions). The loss function minimised to train the affine registration module of the composition network (in a self-supervised manner), and estimate the desired 3D affine transformations is given by,

$$\mathcal{L}_{affine} = \sum_{c=1}^C \|\mathbf{V}_o^{transf} - \mathcal{T}_c \mathbf{V}_c\|_1 \quad (7)$$

where, \mathcal{T}_c represents the affine transformation estimated and applied to part c in the assembly; \mathbf{V}_c denotes the vertices shared between part c and all other $C-1$ parts in the assembly, where the latter (i.e. all other $C-1$ parts) are represented by subscript o . \mathbf{V}_o^{transf} denotes the transformed vertices shared between all other $C-1$ parts in the assembly given the c^{th} part. Here, \mathbf{V}_o^{transf} is constructed by concatenating shared vertices from all $C-1$ parts (given a part c in the assembly), following affine transformation. I.e. $\mathbf{V}_o^{transf} = \{\mathcal{T}_d \mathbf{V}_d\}_{d=\{1..C-1\}}$, where, \mathbf{V}_d denotes the vertices shared between part d in the assembly and part c , for $d \neq c$.

Ensuring coherence at boundaries between adjacent cardiovascular structures is essential to ensure anatomical plausibility in the synthesised *virtual chimaera* cohorts and prevent topological errors in the whole heart shape assemblies. As rigid/affine registration alone is insufficient to prevent intersections, gaps between adjacent cardiovascular structures in the assembly or both; our composition network also comprises a non-rigid registration module which deforms each part locally, and refines the composition of the synthesised structures. The non-rigid registration module is a graph-convolutional neural network with a similar encoder-decoder architecture employed for each part-specific gcVAE in the independent generator, and additional skip connections [44] aggregating the features in each encoder block with its corresponding decoder block at the same mesh resolution level. This module is trained as an autoencoder rather than a VAE. It uses the coarsely-aligned whole heart shape composed by the preceding affine registration step as input. It estimates vertex-wise displacements to refine the spatial composition of the whole-heart shape assembly. The non-rigid registration module is also trained in a self-supervised manner (as with the affine registration module) by minimising a loss function given by,

$$\mathcal{L}_{non-rigid} = \sum_{c=1}^C \|\mathbf{V}_o^{transf} - \mathcal{T}_c^{nr} \mathbf{V}_c\|_1 + \omega_3 \mathcal{L}_{Laplacian} + \omega_4 \|\mathcal{T}_c^{nr}\|_1 \quad (8)$$

where, \mathcal{T}^{nr} represents the non-rigid transformation, i.e. the vertex-wise displacements, estimated for all vertices of all parts in the coarsely aligned full heart shape output from the preceding affine composition step; and \mathcal{T}_c^{nr} are the displacements estimated for the vertices shared between part c (denoted \mathbf{V}_c) and all other $C-1$ parts in the assembly. The shared vertices of the latter (i.e. all other $C-1$ parts) are represented by subscript o and \mathbf{V}_o^{transf} denotes the transformed vertices shared between all other $C-1$ parts in the assembly and the c^{th} part. Here, \mathbf{V}_o^{transf} is constructed by concatenating vertices shared between all $C-1$ parts and the c^{th} part in the assembly, following deformation using the estimated vertex-wise displacements. I.e. $\mathbf{V}_o^{transf} = \{\mathcal{T}_d^{nr} \mathbf{V}_d\}_{d=\{1\dots C-1\}}$, where, \mathbf{V}_d denotes the vertices shared between part d in the assembly and part c , for $d \neq c$. In equation 8, $\mathcal{L}_{Laplacian}$ represents the Laplacian loss (described in equation 4) used to regularise the estimated vertex-wise displacements, encouraging the latter to be similar for neighbouring vertices and resulting in smooth, localised deformations of each part in the shape assembly. The third term in the equation 8 applies L1 normalisation to the vertex-wise displacements to encourage sparsity in the estimated vertex displacements and penalise motion of vertices that are not in the vicinity of vertices shared between two adjacent regions. ω_3 and ω_4 are the regularisation parameters that are tuned empirically.

Following this two-step process, comprising an initial affine and subsequent non-rigid registration step, the composition network is trained by optimising \mathcal{L}_{affine} and $\mathcal{L}_{non-rigid}$, respectively, to spatially organise the cardiovascular structures synthesised by the part-aware generator into anatomically consistent cardiac *virtual chimaeras*.

III. EXPERIMENTS CONFIGURATION

A. Datasets

The generative shape compositional framework proposed in this study was trained and validated using a subset of the cardiac cine-magnetic resonance (cine-MR) imaging data available from the UK BioBank (UKBB) [45]. We created a cohort of 2360 whole-heart subject-specific meshes using the manual contours provided for all four cardiac chambers in a previous study [46]. The whole-heart subject-specific meshes were created by registering a high-resolution cardiac atlas mesh from a previous study [12] to the manual contours. The cardiac atlas comprises the following cardiovascular structures - left/right ventricle (LV/RV), left/right atrium (LA/RA), aorta vessel root, and four valve planes (i.e. mitral, tricuspid, aortic, and pulmonary valves). Additionally, vertices in the atlas mesh are shared between the following pairs of structures - LV-RV, LV-LA, LA-RA, RV-RA, LV-aorta, LA-aorta, and RA-aorta. Registration of the atlas mesh to each subject's manual contours results in a cohort of subject-specific meshes (i.e. undirected graphs) that share point correspondence, i.e. have the same number of vertices/nodes. This enables use of spectral convolutions in the graph-convolution layers used throughout the proposed generative shape compositional framework (as fixed/common graph topology across all samples is a pre-requisite for the former). Additionally, the self-supervised learning scheme proposed in this study to train the composition network is driven by the shared vertex information available for adjacent parts/structures in the cardiac atlas mesh (which is automatically propagated to all subject-specific meshes via registration). Atlas-to-contour registration was achieved using a combination of the point set registration algorithm (viz. generalised coherent point drift) developed previously by our group [47] to establish soft correspondences between atlas and subject-specific contours, and subsequent thin-plate-spline based warping of the atlas mesh to each subjects' contours. Further details on the registration process used to create the cohort of subject-specific meshes used in this study are available in [48]. We randomly split the available cohort of whole heart meshes from 2360 subjects into 422/59/1879 for training, validation and testing, respectively. We explore two distinct scenarios when training the proposed generative shape compositional framework. These include - (a) *complete overlap* in the data across all training samples, i.e. where all subjects' data included in the training set, contain all cardiovascular structures in the whole heart shape assembly; and (b) *partial overlap* in the data across training samples, where, 300 subjects have only one cardiovascular structure, resulting in 60 samples for each of the five structures of interest (i.e. LV, RV, LA, RA, and aorta), while, the remaining 122 subjects in the training set are considered to have complete whole heart shape assemblies. Throughout this study, for each subject, we only use meshes representative of one time point in the cardiac cycle, namely, at end-diastole (ED). The resulting samples in the training, validation, and test sets are used to train and evaluate the proposed approach throughout the study.

B. Implementation Details

The proposed approach was implemented using PyTorch [49], on a PC with an NVIDIA RTX 2080Ti GPU. We trained the part-aware generative models (i.e. both the independent and dependent generator) using the Adam optimiser [50] with an initial learning rate of $1e-4$, and batch size of 16 for 600 epochs. The order of the Chebyshev convolution polynomial was set to 6. The latent dimensions of each part-specific sub-network in the independent generator were set to 16, 12, 16, 12, and 8 for the LV, RV, LA, RA, and aorta, respectively. While, the latent dimension of the dependent generator was set to 60, with 12 components of the latent vector dedicated to modelling the shape variability observed in each of the five cardiovascular structures of interest, namely, LV, RV, LA, RA, and aorta. We set the resampling factors for learning shape features across a multi-resolution mesh hierarchy to: [4, 4, 4, 6, 6] for the LV and RV, [4, 4, 4, 4, 5] for the LA, [4, 4, 4, 4, 6] for the RA, and [4, 4, 4, 4, 4] for the aorta. These down- and up-sampling factors were chosen empirically for the five graph-convolution blocks in the encoder and decoder networks, respectively, in both the independent and dependent generator. While training the independent and dependent generator, a warm-up strategy was adopted to improve stability and prevent mode collapse in the learned posterior distribution over the latent variables. This is achieved by initially training the part-wise gcVAEs in the independent generator, and the mcVAE in the dependent generator, with the weight of KL loss term (i.e. ω_0 in equation 1) set to zero for 300 epochs (i.e. they are trained as plain autoencoders). The learned weights initialise the subsequent training step for the independent and dependent generator, wherein, the weight of the KL loss term is initially set to a small value, i.e. $1e^{-6}$, and subsequently increased each epoch by multiplying by a factor of 1.25, up to a maximum value of $1e^{-4}$. The weight for the other regularisation terms in the composite loss function (refer to equation 6), namely, ω_1 and ω_2 were set to 8 and 1. While, the weights for the regularisation terms in the self-supervised registration loss function (refer to equation 8) used to train the composition network, namely, ω_3 and ω_4 , were set to 8 and $5e^{-7}$, respectively.

The hyperparameters of the network architecture and optimiser used for the part-aware generator were retained for the composition network, with except for the initial learning rate and the batch size, which were set to $5e^{-4}$ and 4, respectively. We randomly sampled individual part shapes from different patients to train the composition network. This helped demonstrate that the proposed composition network can be trained with *partially overlapping* data. First, the composition network was pre-trained using parts sampled from the original patient-specific cardiac meshes for 100 epochs. The data splits used to train and evaluate the part-aware generative models were kept the same for the composition network to ensure fair evaluation. Subsequently, we fine-tuned the composition network for 200 epochs using parts synthesised by the IG-CO part-aware generative model. The dataset of synthesised parts comprised 2000 samples, randomly split into 1600/200/200 for training, validation, and testing, respectively.

All hyperparameters associated with both the part-aware generative models and the composition network were tuned based on the validation set. The performance of the proposed generative shape composition framework was evaluated on the held-out test set, using several metrics designed to assess model generalisability, specificity, and the plausibility in key clinical cardiac indices across synthesised *virtual chimaera* cohorts (relative to the real UK Biobank population).

C. Generating Virtual chimaera Cohorts

When developing/choosing generative shape models for any given application, and sampling strategies used to synthesise virtual cohorts of anatomy from the former, it is typical to make design choices that achieve a balance/trade-off between the variability in shape captured (relative to target/real patient populations). The anatomical plausibility of the instances synthesised, in the virtual cohorts. Balancing shape variability and anatomical plausibility in synthesised virtual cohorts is essential for *in-silico* trials as cohorts with large variability may contain unrealistic shapes, unrepresentative of native anatomy/naturally occurring variations. Conversely, cohorts synthesised with strict plausibility constraints may not be expressive in the range of shape variations they represent, limiting the anatomical envelope that can be explored in subsequent *in-silico* trials. A thorough quantitative assessment of the benefits and drawbacks of applying different sampling strategies to PCA-based shape models was explored in [26], in the context of synthesising virtual cohorts of the aortic root and vessel. Romero et al. concluded that uniform sampling in the learned latent space/principal sub-space of a shape model yields cohorts with greater shape variability, while sampling from unit Gaussian distributions to generate latent vectors representative of virtual shape instances (for PCA-based shape models), ensures greater plausibility in the synthesised virtual cohorts. Most existing studies generate new samples by sampling from the unit Gaussian distribution [33], [51]. In this study, we favour the synthesis of cohorts in a manner that maximises the variability in shape captured for each cardiac structure of interest, and therefore, opt for a uniform sampling strategy to synthesise cardiac *virtual chimaeras*. The rationale for doing so was to assess whether virtual cohorts were synthesised using the different generative shape models investigated in this study, capture the variability in cardiac shape and associated clinically relevant cardiac indices, observed in a real (and unseen) population. Specifically, using the generative shape models proposed in this study (i.e. the independent and dependent generator) we synthesise cardiac *virtual chimaera* cohorts by uniformly sampling each latent variable within the interval of mean ± 2 standard deviations, where the means and standard deviations for each latent variable are learned from the training data. Similarly, for fair comparison, virtual cohorts are synthesised using the PCA-based shape model by sampling coordinates in the low-dimensional principal sub-space uniformly in the interval defined $[-2\sqrt{\lambda_i}, +2\sqrt{\lambda_i}]$, where, λ_i denotes the eigenvalue of the i^{th} principal component (i.e. i^{th} eigenvector spanning the principal sub-space). The PCA-based shape model used

throughout this study retained 24 principal components as they explained 95% of the variation in cardiac shapes observed in the training set used for all models. Additionally, when sampling latent vectors/coordinates in principal sub-space, two standard deviations about the mean were used throughout as we experimentally verified that that sampling with three standard deviations or more resulted in a large number of irregular/implausible shapes in the synthesised virtual cohorts.

D. Evaluation Criteria

We evaluated the proposed generative shape compositional framework in terms of the following criteria: generalisability, which measures the ability of trained shape models to reconstruct unseen cardiac shapes, and thereby, assesses the variability in shape captured by the learned latent representations; specificity, which assesses anatomical plausibility in the cardiac virtual cohorts synthesised; and clinical relevance. Generalisation errors were evaluated using the Euclidean distance (ED) and F1-score [52], [53]. Specifically, unseen test shapes were first reconstructed using the trained shape models investigated in this study, i.e. PCA, IG-CO, IG-PO, DG-CO and DG-PO. Subsequently, the ED and F1-score were evaluated between the original and reconstructed test shapes. Specificity errors meanwhile, were quantified as the ED between each sample in the synthesised virtual populations and its nearest neighbour (in terms of ED) in the unseen real population of cardiac shapes. ED was evaluated as the vertex-to-vertex euclidean distance between any two cardiac shapes. The F1-score computes the precision and recall by checking the ratio of points in prediction or ground truth that can find a nearest neighbor from the others within a certain threshold. Furthermore, registration errors incurred by the composition network were quantified using the Hausdorff distance (HD). Specifically, HD was used to measure the distance between vertices shared across all pairs of adjacent cardiac chambers with shared boundaries, following affine and non-rigid composition.

IV. RESULTS

We conducted several experiments to evaluate the performance of the generative shape models proposed in this study, and compared them against each other and PCA. This section summarises the results obtained in terms of generalisation and specificity errors obtained for the methods investigated, and the quality of their synthesised cardiac virtual populations, assessed in terms of key clinical cardiac indices.

A. Generalisability

A model with good generalisability can capture the variability of the seen (training) data and generalise to, or explain, unseen (testing) data. The generalisability of a generative/statistical shape model can be assessed in terms of the error incurred when reconstructing unseen test data, thus assessing its ability to explain unseen shapes and providing insights to the overall variability in shape captured by the model [54]. Table I summarises the generalisation errors of

all methods investigated in this study, for all five cardiovascular structures of interest. We observe that the IG models significantly outperform PCA for three of the five structures of interest (i.e. LV, LA and RA). Of particular importance to note is that IG-PO, which was trained with missing/partially overlapping data, also outperformed PCA, which conversely, was trained with complete data. Additionally, both IG models consistently outperformed the DG models in generalisation errors, across all five structures. This indicates that by learning an independent part-specific latent space, the IG models can capture a greater degree of shape variability for each structure of interest than afforded by PCA, and correspondingly can synthesise more diverse (in terms of shape) virtual cardiac populations than the latter. Examples of cardiac virtual chimaeras generated by spatially composing (using the composition network) individual parts/structures sampled from the trained IG-CO model are shown in Figure 3.

B. Specificity

Specificity errors are used to quantitatively assess anatomical plausibility of the synthesised cardiac virtual populations. This is done by evaluating the distance of each generated sample in the virtual population to the closest/most similar shape in the real population [54]. Table II summarises the specificity errors obtained for the cardiac virtual populations synthesised using each model investigated. Errors are quantified for each of the five structures of interest individually, and the whole heart shape assemblies. We observe that both DG-CO achieves the highest specificity (i.e. lower specificity errors) of all methods investigated, across all structures except the aorta. While, DG-PO, which was trained with *missing parts/partially overlapping* data, is comparable to PCA across all structures. By learning a joint latent representation across all parts in the whole heart shape assemblies, the dependent generator models constrain the posterior distribution of the latent variables to explain shared variation across multiple parts. Intuitively, this enforces a greater degree of plausibility in the whole heart shape instances generated from the trained model.

Conversely, the independent generator model IG-CO, trained using *complete data* has lower specificity (i.e. higher specificity errors) than PCA and the dependent generator models for the ventricles but is comparable to the latter for the atria. As the independent generator models learn distinct latent representations for each part/structure, co-variation in shape across multiple parts is not captured. Consequently, the learned part-wise latent spaces focus on maximally capturing the variability in shape of each part, at the cost of plausibility in the instances generated.

C. Evaluation of clinical relevance

Based on the evaluation criteria proposed in [26] for assessing the clinical relevance of aortic vessel virtual cohorts synthesised by generative shape models, we assess the clinical relevance of the cardiac virtual cohorts synthesised using the models investigated in this study. Specifically, we define the clinical acceptance rate (\mathcal{A}) as the percentage of synthesised

TABLE I

GENERALISATION ERRORS OF OUR PROPOSED INDEPENDENT/DEPENDENT GENERATOR TRAINED ON COMPLETE/PARTIAL OVERLAPPING DATASET AND PCA MODEL IN THE HOLD-OUT TEST DATASET (MEAN \pm STD). THE **BOLD** RESULTS REPRESENT THEIR PERFORMANCES ARE SIGNIFICANTLY BETTER THAN THOSE OF PCA MODELS.

Part	PCA		Dependent Generator				Independent Generator			
			Complete		Partial		Complete		Partial	
	ED	F1	ED	F1	ED	F1	ED	F1	ED	F1
LV	2.37 \pm 0.71	0.71 \pm 0.11	1.78\pm0.38	0.72\pm0.66	1.92\pm0.39	0.70 \pm 0.11	0.88\pm0.17	0.95\pm0.05	1.43\pm0.25	0.82\pm0.08
RV	1.74 \pm 0.39	0.82 \pm 0.07	2.68 \pm 0.55	0.66 \pm 0.08	2.76 \pm 0.61	0.65 \pm 0.09	1.84 \pm 0.62	0.75 \pm 0.15	2.22 \pm 0.55	0.71 \pm 0.11
LA	2.10 \pm 0.51	0.82 \pm 0.07	2.70 \pm 0.62	0.71 \pm 0.09	2.51 \pm 0.57	0.73 \pm 0.09	1.47\pm0.41	0.89\pm0.08	1.84\pm0.50	0.83\pm0.09
RA	1.43 \pm 0.37	0.92 \pm 0.05	1.99 \pm 0.61	0.82 \pm 0.10	2.15 \pm 0.62	0.80 \pm 0.10	1.21\pm0.40	0.93\pm0.09	1.43\pm0.49	0.90 \pm 0.09
Aorta	1.40 \pm 0.40	0.92 \pm 0.06	1.98 \pm 0.55	0.80 \pm 0.10	2.18 \pm 0.67	0.77 \pm 0.12	1.51 \pm 0.48	0.87 \pm 0.11	1.71 \pm 0.45	0.83 \pm 0.10
Full Heart	2.30 \pm 0.74	0.77 \pm 0.08	3.53 \pm 0.76	0.66 \pm 0.07	3.48 \pm 0.71	0.66 \pm 0.06	2.97 \pm 0.73	0.71 \pm 0.08	3.18 \pm 0.75	0.69 \pm 0.08



Fig. 3. Examples of *virtual chimaeras* generated by the independent generator trained with *complete data* (IG-CO). Each component of the latent vector was randomly sampled from the posterior Gaussian distribution learned from training dataset.

TABLE II

SPECIFICITY ERRORS OF THE VIRTUAL POPULATIONS FROM DIFFERENT MODELS (MEAN \pm STD). THE **BOLD** RESULTS REPRESENT THEIR SPECIFICITY ARE SIGNIFICANTLY BETTER THAN OR HAVE NO SIGNIFICANT DIFFERENCE WITH THOSE OF PCA MODELS.

Methods	Full Heart	LV	RV	LA	RA	aorta
PCA	3.262 \pm 0.007	2.211 \pm 0.006	2.687 \pm 0.009	2.688 \pm 0.010	3.054 \pm 0.011	2.217 \pm 0.008
DG-CO	3.160\pm0.007	1.974\pm0.006	2.647\pm0.006	2.524\pm0.008	2.958\pm0.013	2.399 \pm 0.013
DG-PO	3.325\pm0.017	2.219\pm0.025	2.640\pm0.020	2.598\pm0.009	3.058\pm0.020	2.254 \pm 0.015
IG-CO	3.780 \pm 0.073	2.558 \pm 0.064	3.668 \pm 0.122	2.731\pm0.044	3.094\pm0.048	2.555 \pm 0.053
IG-PO	3.353 \pm 0.006	2.181\pm0.005	2.653\pm0.008	2.712\pm0.007	3.150 \pm 0.011	2.312 \pm 0.008

samples in the virtual cohorts whose cardiac indices, namely, LV Volume, RV Volume, LA Volume, and RA Volume, lie within a 90% confidence interval of the distribution of these indices, observed in the UK Biobank population considered in this study. As the distributions of these indices were verified to be non-Gaussian using the Kolmogorov-Smirnov test, we rely on Chebyshev's inequality to define the 95% confidence interval based on the corresponding mean (μ), variance (σ^2) and the mode (M) observed in a real-world population. According to Chebyshev's inequality, intervals defined by $M \pm 2B$, where

$B = \sqrt{\sigma^2 + (M - \mu)^2}$, contain at least 90% of the area under the corresponding probability density functions [55].

Clinical acceptance rate \mathcal{A} is used as an additional metric to assess anatomical plausibility of the synthesised virtual cohorts. It is motivated by the need to preserve clinically relevant cardiac volumetric indices in the synthesised cohorts (relative to the reference real UK Biobank population). Table III summarises the statistical description of each cardiac index in the whole population and \mathcal{A} calculated for all four cardiac chambers in the synthesised virtual cohorts. The dependent

TABLE III
CLINICAL ACCEPTANCE RATE $\mathcal{A}(\%)$ FOR CARDIAC VIRTUAL COHORTS SYNTHESISED USING ALL METHODS INVESTIGATED.

Cardiac Indices	μ	σ	M	$M \pm 2B$	PCA	Dependent Generator		Independent Generator	
						Complete	Partial	Complete	Partial
LV-Volume	131.94	20.39	127.06	[85.12, 168.99]	98.05	100	96.95	98.15	99.90
RV-Volume	116.75	20.66	118.19	[76.77, 159.61]	93.50	99.50	98.30	90.50	97.30
LA-Volume	34.98	9.78	30.69	[9.33, 52.04]	84.60	98.90	98.50	94.85	99.65
RA-Volume	52.39	10.87	47.93	[24.43, 71.43]	87	95.40	97.25	96.65	99.10

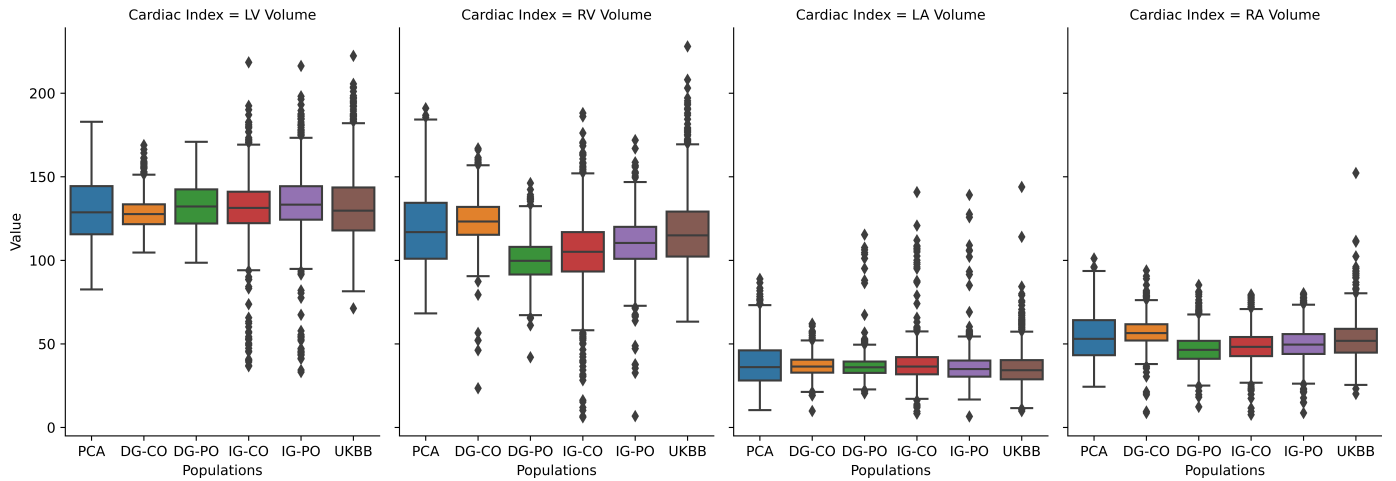


Fig. 4. Box plots compare the median and interquartile range for all four cardiac indices of interest across the synthesised virtual cohorts and the UK Biobank population. Boxplots for each virtual cohort synthesised are labelled according to the corresponding method used, namely: PCA, IG-CO, IG-PO, DG-CO and DG-PO.

generator models (DG-CO and DG-PO) obtain the highest acceptance rates across most cardiac indices (except for LA-volume for DG-PO), which is consistent with the specificity errors summarised in Table II. Although the specificity errors indicate that the independent generator models synthesise cardiac chamber shapes that are less plausible than PCA in some cases, the clinical acceptance rates estimated for both IG-CO and IG-PO are consistently higher than PCA across all cardiac indices (refer to Table III). This indicates that the independent and dependent generator models proposed in this study, when trained with *complete* and *partially overlapping* data, provide better fidelity in preserving the distributions of clinically relevant cardiac indices in the synthesised virtual cohorts relative to the UK Biobank population, than PCA. The range of values estimated for all four cardiac indices of interest, namely, LV-volume, RV-volume, LA-volume and RA-volume, across all synthesised virtual cohorts and the real UK Biobank population considered in this study, are summarised as boxplots in Figure 4.

D. Evaluation of non-rigid spatial composition

A key contribution in this study is the formulation of a self-supervised non-rigid composition network to spatially compose synthesised cardiovascular structures into coherent whole heart shape assemblies (viz. cardiac *virtual chimaeras*). While previous approaches to generative shape composition learning have proposed rigid/affine composition networks, this is the first study to adopt non-rigid registration for the same (in addition to estimating an initial affine transformation). To

demonstrate the benefits of the composition network's non-rigid registration component, we compared the quality of the composed cardiac *virtual chimaeras* obtained using just affine registration with those obtained using affine and non-rigid registration. Data from the held out test set and samples from the virtual cohort synthesised using IG-CO were used in this experiment. Table IV summarises the Hausdorff distance (HD) between the shared vertices of all seven pairs of adjacent structures in the whole heart shape assemblies with shared boundaries, after composition with (w/) and without (w/o) non-rigid registration. These results indicate that the non-rigid spatial composition network consistently outperforms its affine counterpart across all adjacent structures, achieving significantly lower HD errors (reported as mean \pm std calculated across all samples N used in the experiment, refer to Table IV). Non-rigid registration is thus a key component for synthesising cardiac *virtual chimaeras* using the proposed framework as it improves coherence at boundaries between adjacent structures and reduces topological defects, relative affine registration alone.

V. DISCUSSION

In this study, a novel generative shape compositional framework is presented for synthesising cardiac virtual populations. While several previous studies have proposed generative shape models for synthesising virtual populations of multi-part anatomical shapes, they have all relied on the availability of training data with *complete overlap* across all samples, i.e. all structures/parts of interest being available across all

TABLE IV

HAUSDORFF DISTANCES (MEAN \pm STD) ESTIMATED BETWEEN SHARED VERTICES OF ALL PAIRS OF ADJACENT STRUCTURES WITH SHARED BOUNDARIES IN THE WHOLE HEART SHAPE ASSEMBLIES. WHOLE HEART SHAPE ASSEMBLIES WERE COMPOSED USING THE SPATIAL COMPOSITION NETWORK WITH (W/) AND WITHOUT (W/O) NON-RIGID REGISTRATION, BASED ON DATA FROM: (A) THE HELD OUT TEST DATASET WHICH WAS RECONSTRUCTED USING IG-CO; AND (B) PARTS/STRUCTURES SYNTHESISED BY THE TRAINED IG-CO MODEL.

Adjacent Structures	Reconstructed (N=1879)		Synthesised (N=200)	
	w/o (mm)	w/ (mm)	w/o (mm)	w/ (mm)
LV-RV	6.30 \pm 1.61	1.69 \pm 0.42	7.90 \pm 5.87	2.53 \pm 3.44
LV-LA	5.09 \pm 1.35	1.51 \pm 0.32	6.17 \pm 6.06	1.94 \pm 2.27
LA-RA	4.26 \pm 1.22	1.26 \pm 0.28	4.78 \pm 1.37	1.40 \pm 0.54
RV-RA	5.74 \pm 1.67	1.39 \pm 0.29	6.55 \pm 2.99	1.67 \pm 1.24
LV-aorta	4.49 \pm 1.24	1.40 \pm 0.28	5.54 \pm 6.24	2.15 \pm 3.92
LA-aorta	2.97 \pm 1.04	0.88 \pm 0.20	3.20 \pm 1.22	1.08 \pm 0.94
RA-aorta	5.09 \pm 1.43	1.66 \pm 0.43	6.25 \pm 2.11	2.23 \pm 0.94

samples in the training set. Consequently, existing approaches are not designed to combine the shape information available in *partially overlapping* data, i.e. individual structures/parts from different samples/patients, and synthesise complete multi-part shape assemblies. Leveraging *partially overlapping* data is especially useful in scenarios where it is necessary to combine information from disparate multi-modal data sets to enrich the training set and capture the desired variability in shape of multi-part shape assemblies. The two generative models introduced within the shape compositional framework proposed in this study, namely, the independent and dependent generators, were demonstrated to synthesise plausible whole-heart shape assemblies using *partially overlapping* training data. The specificity of both the IG-PO and DG-PO models were comparable to or better than PCA, where the latter was trained with *complete* data. In addition to synthesising plausible shape instances, generative shape models should generalise well to unseen shape instances, which is also indicative of the variability in shape (observed in the training population) captured by the trained models. Generalisation errors evaluated for the models investigated in this study highlight the ability of IG-PO to generalise to unseen shapes better than PCA, for three out of the five cardiovascular structures of interest (i.e. LV, LA and RA).

Furthermore, the clinical relevance of the virtual cohorts synthesised using all methods investigated in this study were assessed in terms of the preservation of key cardiac volumetric indices, relative to the observed real UK Biobank population. The metric used for the same, namely, the clinical acceptance rate (refer to section IV-C) highlighted the ability of all four models investigated within the proposed generative shape compositional framework (i.e. IG-CO, IG-PO, DG-CO and DG-PO) to preserve clinically relevant cardiac indices within a 90% interval of the values observed in the real population, in a greater proportion of their virtual cohort samples, than afforded by PCA. This helps further demonstrate the ability of the proposed shape compositional framework to generate better quality cardiac virtual cohorts than PCA, even in the presence of *missing/partially overlapping* training data.

PCA-based statistical shape modeling is a powerful tool for synthesising virtual populations of anatomical struc-

tures [11] and has been explored extensively for this purpose in several previous studies [12], [26]. However, a fundamental limitation of PCA-based SSMs' inability is to learn latent/low-dimensional shape representations from *missing/partially overlapping* training data. Thus, such models require all parts/structures to be available for samples in the training population to synthesise complete multi-part shape assemblies (e.g. whole heart shapes considered in this study). Additionally, PCA-based models are linear projections of shape data on to a lower-dimensional sub-space and cannot effectively capture non-linear variations in shapes. This results in limited generalisation capacity and specificity for statistical shape models trained using such approaches, and correspondingly, limits the anatomical plausibility of synthesised virtual cohorts. gcVAE-based generative shape models on the other hand, can capture non-linear variations in shapes, yielding virtual cohorts with higher specificity/anatomical plausibility (see Tables II and III) and generalising better to unseen shapes (refer to Table I). Amongst the gcVAE-based shape models investigated in this study, the dependent generator models (DG-CO and DG-PO) are based on a graph convolutional multi-channel VAE [35], which can capture non-linear correlations between all cardiovascular structures of interest, by learning a shared latent space across all structures. This enables the dependent generator models to generate virtual cohorts with better specificity/anatomical plausibility than the independent generator models (refer to Table II). Higher specificity of the dependent generator models is further complemented by their ability to better preserve key cardiac clinical indices in the synthesised virtual cohorts than their independent generator counterparts, as evidenced by the higher clinical acceptance rates achieved for each relevant cardiac index evaluated (refer to Table III). Improved specificity however, comes at the cost of generalisability and the overall variability in shape captured by the dependent generator models as the learned latent space is constrained to explain the shared variation of all structures in the whole heart shape assemblies observed across the training population.

Conversely, the independent generator models do not capture correlations between structures as they use independent part-wise VAEs, however, their dedicated part-wise latent spaces provide greater flexibility than their dependent generator counterparts, enabling them to capture a greater degree of variability in shape for the structures of interest. This is reflected in the lower generalisation errors achieved by the independent generator models (see Table I), and the wider range of values observed for relevant cardiac indices in the synthesised virtual cohorts (refer to Figure 4), relative to their dependent generator counterparts. The relative merits identified for the independent and dependent generator models proposed in this study indicate that for conducting *in-silico* trials using virtual cohorts synthesised by either approach, the following broad generalisations can be made regarding their suitability/applicability in different scenarios - the dependent generator model and cardiac *virtual chimaera* cohorts synthesised thereof, are better suited to ISTs where greater statistical fidelity is required in the enrolled virtual patients/*chimaeras*, in terms of key/relevant anatomical phenotypes. For example,

ISTs where the aim is to evaluate the safety and efficacy of a medical device in a specific target patient population; and conversely, the independent generator model is better suited to exploratory ISTs, where the aim is to investigate 'what if' scenarios and assess the performance of medical devices in niche sub-populations that express phenotypic traits that are concentrated in the tails of the general population distribution, i.e. in other words, where, virtual cohorts with greater anatomical variability are desired.

Previous studies on generative shape composition learning [31], [32] within the computer vision domain have relied on fully supervised learning to spatially compose synthesised parts into multi-part shape assemblies, by estimating rigid or affine transformations. The multi-part shape assemblies utilised in these studies typically comprise rigid constituent parts/structures (e.g. chairs, tables, airplanes, etc.). However, soft tissue anatomical structures are deformable and exhibit significant non-linear variations in shape across individuals in a population. Consequently spatially composing multiple such structures into anatomically plausible shape assemblies requires both affine and non-rigid registration. In other words, generative shape composition learning for multi-part/multi-organ structures requires the synthesised structures to be treated as a recomposable set of deformable parts. We address this challenge by introducing a self-supervised affine and non-rigid spatial composition network, alleviating the need for ground truth transformations and/or composed multi-part shape assemblies to be available *a priori*. As shown in Table IV, the non-rigid registration component of the proposed spatial composition network yields significant improvements over its purely affine counterpart, in terms of the coherence achieved at shared boundaries between adjacent structures in the composed whole heart shape assemblies. Furthermore, the self-supervised learning approach used to train the spatial composition network is driven by weak labels defined by the shared vertices between all pairs of adjacent structures with shared boundaries. Hence, the composition network can be trained with parts/structures that are synthesised independently of each other. This is central to enabling the proposed generative shape composition framework to be trained with *partially overlapping* data (i.e. where the training population comprises patients' data with missing parts/structures).

Although the proposed approach facilitates synthesis of cardiac virtual cohorts using missing/partially overlapping training data, some limitations and potential for future improvements remain. For example, the current generative shape compositional framework requires all input shapes, represented as surface meshes, to share point-wise correspondence and comprise the same graph topology (i.e. mesh triangle connectivity should be identical). This requires co-registration of all corresponding parts' meshes for all patients included in the training, validation and test populations before training or evaluating any of the components of the proposed framework. This co-registration pre-processing step helps establish point-wise spatial correspondence and maintain a fixed graph topology across all samples, but also limits the utility of the proposed generative shape compositional approach to those applications where anatomical shape correspondence exists and

can be estimated. This precludes the application of the present framework from modeling organs' shapes where pathology-driven topological changes are present and diverse across patient populations (as there is no notion of anatomical correspondence in such a scenario). Expanding the current approach to accommodate variable topology in anatomical structures across patients/input samples, and synthesising anatomically plausible virtual populations, would broaden the range of applications in computational medicine and *in-silico* trials that the approach would be suitable for. The current generative shape compositional framework does not guarantee that the topology of the synthesised virtual chimaeras are preserved, relative to native anatomy, as no explicit constraint enforces the same. Although the spatial composition network achieves low errors following alignment/composition of individual cardiac structures into a whole-heart shape assembly, minor topological defects such as localised intersections/holes between adjacent structures remain in some virtual chimaera instances. In the context of conducting *in-silico* trials using cardiac virtual chimaera cohorts synthesised by the proposed approach, these topological errors must be fixed using appropriate mesh/geometry processing techniques (which is feasible), before computational volumetric meshes that are usable in biomechanistic simulations can be created from the same. Such issues may be addressed by introducing additional geometric and/or topological constraints to the learning process, which we will explore in future work. Finally, the current study only emulates the scenario of learning to synthesise whole-heart shape assemblies using missing/partially overlapping training data from different patients/patient populations (i.e. only UK Biobank data is used throughout this study). Future work will explore combining anatomical structures extracted from multi-modal imaging data, acquired across different patient populations (e.g. aortic vessel from CTA available from a clinical trial and left ventricle from cine-MRI available in UK Biobank), to synthesise cardiac virtual chimaera cohorts.

VI. CONCLUSION

A generative shape modeling framework is proposed in this study for building cardiac virtual populations. A key contribution of the study is to treat the task of synthesising multi-part objects, such as whole-heart shape assemblies, as one of generative shape composition learning. The proposed approach can synthesise complete whole heart shape assemblies, using *partially overlapping* training data, i.e. where, all the cardiovascular structures of interest are not available for all patients that constitute the training population. This demonstrates its potential for combining *partially overlapping* anatomical structures from disparate databases and patient populations, to synthesise anatomically plausible cardiac virtual cohorts. We explore two generative shape modeling schemes within the proposed framework: the independent generator and the dependent generator. The former facilitates generation of more diverse cardiac virtual cohorts, in terms of variability in shapes of cardiovascular structures and their corresponding clinically relevant volumetric indices. The latter provides greater statistical fidelity, resulting in more anatomically plausible cardiac virtual cohorts. Although synthesis of

cardiac virtual cohorts is the focus of this proof-of-concept study, the proposed generative shape compositional framework is generic. It may be employed to synthesise virtual cohorts of other multi-part organs or multi-organ ensembles (e.g. lungs and their associated airways, abdominal organs, the complete spine, etc.). This study is an important step towards integrating anatomical shape information from disparate, multi-modal datasets, and diverse patient populations, to synthesise cardiac *virtual chimaera* cohorts suitable for conducting *in-silico* trials of medical devices.

REFERENCES

- [1] M. Viceconti, F. Pappalardo, B. Rodriguez, M. Horner, J. Bischoff, and F. M. Tshinanu, "In silico trials: Verification, validation and uncertainty quantification of predictive models used in the regulatory evaluation of biomedical products," *Methods*, vol. 185, pp. 120–127, 2021.
- [2] K. Madan, "Natural human chimeras: A review," *European Journal of Medical Genetics*, vol. 63, no. 9, p. 103971, 2020.
- [3] M. Niemeyer and A. Geiger, "Giraffe: Representing scenes as compositional generative neural feature fields," in *Proceedings of the IEEE/CVF Conference on Computer Vision and Pattern Recognition*, 2021, pp. 11453–11464.
- [4] J. Cao, O. Katzir, P. Jiang, D. Lischinski, D. Cohen-Or, C. Tu, and Y. Li, "Dida: Disentangled synthesis for domain adaptation," *arXiv preprint arXiv:1805.08019*, 2018.
- [5] T. Heimann and H.-P. Meinzer, "Statistical shape models for 3d medical image segmentation: a review," *Medical image analysis*, vol. 13, no. 4, pp. 543–563, 2009.
- [6] T. F. Cootes, C. J. Taylor, D. H. Cooper, and J. Graham, "Active shape models-their training and application," *Computer vision and image understanding*, vol. 61, no. 1, pp. 38–59, 1995.
- [7] N. Ravikumar, A. Gooya, S. Çimen, A. F. Frangi, and Z. A. Taylor, "Group-wise similarity registration of point sets using student's t-mixture model for statistical shape models," *Medical image analysis*, vol. 44, pp. 156–176, 2018.
- [8] A. Gooya, C. Davatzikos, and A. F. Frangi, "A bayesian approach to sparse model selection in statistical shape models," *SIAM Journal on Imaging Sciences*, vol. 8, no. 2, pp. 858–887, 2015.
- [9] K.-k. Shen, J. Fripp, F. Mériaudieu, G. Chételat, O. Salvado, P. Bourgeat, A. D. N. Initiative *et al.*, "Detecting global and local hippocampal shape changes in alzheimer's disease using statistical shape models," *Neuroimage*, vol. 59, no. 3, pp. 2155–2166, 2012.
- [10] I. Castro-Mateos, J. M. Pozo, M. Pereañez, K. Lekadir, A. Lazary, and A. F. Frangi, "Statistical interspace models (sims): application to robust 3d spine segmentation," *IEEE transactions on medical imaging*, vol. 34, no. 8, pp. 1663–1675, 2015.
- [11] A. A. Young and A. F. Frangi, "Computational cardiac atlases: from patient to population and back," *Experimental physiology*, vol. 94, no. 5, pp. 578–596, 2009.
- [12] C. Rodero, M. Strocchi, M. Marciniak, S. Longobardi, J. Whitaker, M. D. O'Neill, K. Gillette, C. Augustin, G. Plank, E. J. Vigmond *et al.*, "Linking statistical shape models and simulated function in the healthy adult human heart," *PLoS computational biology*, vol. 17, no. 4, p. e1008851, 2021.
- [13] M. Pereañez, K. Lekadir, X. Albà, P. Medrano-Gracia, A. A. Young, and A. Frangi, "Patient metadata-constrained shape models for cardiac image segmentation," in *Statistical Atlases and Computational Models of the Heart*. Springer, 2015, pp. 98–107.
- [14] X. Alba, M. Pereañez, C. Hoogendoorn, A. J. Swift, J. M. Wild, A. F. Frangi, and K. Lekadir, "An algorithm for the segmentation of highly abnormal hearts using a generic statistical shape model," *IEEE transactions on medical imaging*, vol. 35, no. 3, pp. 845–859, 2015.
- [15] R. Attar, M. Pereañez, A. Gooya, X. Alba, L. Zhang, M. H. de Vila, A. M. Lee, N. Aung, E. Lukaschuk, M. M. Sanghvi *et al.*, "Quantitative cmr population imaging on 20,000 subjects of the uk biobank imaging study: Lv/rv quantification pipeline and its evaluation," *Medical image analysis*, vol. 56, pp. 26–42, 2019.
- [16] G. Bernardino, O. Benkarim, M. Sanz-de la Garza, S. Prat-González, A. Sepulveda-Martínez, F. Crispí, M. Sitges, C. Butakoff, M. De Craene, B. Bijnens *et al.*, "Handling confounding variables in statistical shape analysis-application to cardiac remodelling," *Medical image analysis*, vol. 65, p. 101792, 2020.
- [17] P. Lamata, M. Lazdam, A. Ashcroft, A. J. Lewandowski, P. Leeson, and N. Smith, "Computational mesh as a descriptor of left ventricular shape for clinical diagnosis," in *Computing in Cardiology 2013*. IEEE, 2013, pp. 571–574.
- [18] A. F. Frangi, D. Rueckert, J. A. Schnabel, and W. J. Niessen, "Automatic construction of multiple-object three-dimensional statistical shape models: Application to cardiac modeling," *IEEE transactions on medical imaging*, vol. 21, no. 9, pp. 1151–1166, 2002.
- [19] S. Ordas, E. Oubel, R. Sebastian, and A. F. Frangi, "Computational anatomy atlas of the heart," in *2007 5th International Symposium on Image and Signal Processing and Analysis*. IEEE, 2007, pp. 338–342.
- [20] S. Faghil Roohi and R. Aghaeizadeh Zoroofi, "4d statistical shape modeling of the left ventricle in cardiac mr images," *International journal of computer assisted radiology and surgery*, vol. 8, no. 3, pp. 335–351, 2013.
- [21] D. Perperidis, R. Mohiaddin, and D. Rueckert, "Construction of a 4d statistical atlas of the cardiac anatomy and its use in classification," in *International Conference on Medical Image Computing and Computer-Assisted Intervention*. Springer, 2005, pp. 402–410.
- [22] C. Hoogendoorn, F. M. Sukno, S. Ordás, and A. F. Frangi, "Bilinear models for spatio-temporal point distribution analysis," *International Journal of Computer Vision*, vol. 85, no. 3, pp. 237–252, 2009.
- [23] G. Harshvardhan, M. K. Gourisaria, M. Pandey, and S. S. Rautaray, "A comprehensive survey and analysis of generative models in machine learning," *Computer Science Review*, vol. 38, p. 100285, 2020.
- [24] M. Beetz, A. Banerjee, and V. Grau, "Generating subpopulation-specific biventricular anatomy models using conditional point cloud variational autoencoders," in *International Workshop on Statistical Atlases and Computational Models of the Heart*. Springer, 2021, pp. 75–83.
- [25] S. Niederer, Y. Aboelkassem, C. D. Cantwell, C. Corrado, S. Coveney, E. M. Cherry, T. Delhaas, F. H. Fenton, A. Panfilov, P. Pathmanathan *et al.*, "Creation and application of virtual patient cohorts of heart models," *Philosophical Transactions of the Royal Society A*, vol. 378, no. 2173, p. 20190558, 2020.
- [26] P. Romero, M. Lozano, F. Martínez-Gil, D. Serra, R. Sebastián, P. Lamata, and I. García-Fernández, "Clinically-driven virtual patient cohorts generation: An application to aorta," *Frontiers in Physiology*, p. 1375, 2021.
- [27] R. Bonazzola, N. Ravikumar, R. Attar, E. Ferrante, T. Syeda-Mahmood, and A. F. Frangi, "Image-derived phenotype extraction for genetic discovery via unsupervised deep learning in cmr images," in *International Conference on Medical Image Computing and Computer-Assisted Intervention*. Springer, 2021, pp. 699–708.
- [28] M. Danu, C.-I. Nita, A. Vizitiu, C. Suciu, and L. M. Itu, "Deep learning based generation of synthetic blood vessel surfaces," in *2019 23rd International Conference on System Theory, Control and Computing (ICSTCC)*. IEEE, 2019, pp. 662–667.
- [29] D. P. Kingma and M. Welling, "Auto-encoding variational bayes," *arXiv preprint arXiv:1312.6114*, 2013.
- [30] I. Goodfellow, J. Pouget-Abadie, M. Mirza, B. Xu, D. Warde-Farley, S. Ozair, A. Courville, and Y. Bengio, "Generative adversarial nets," *Advances in neural information processing systems*, vol. 27, 2014.
- [31] J. Li, C. Niu, and K. Xu, "Learning part generation and assembly for structure-aware shape synthesis," in *Proceedings of the AAAI Conference on Artificial Intelligence*, vol. 34, no. 07, 2020, pp. 11362–11369.
- [32] S. Li, M. Liu, and C. Walder, "Editvae: Unsupervised part-aware controllable 3d point cloud shape generation," *arXiv preprint arXiv:2110.06679*, 2021.
- [33] A. Ranjan, T. Bolkart, S. Sanyal, and M. J. Black, "Generating 3d faces using convolutional mesh autoencoders," in *Proceedings of the European Conference on Computer Vision (ECCV)*, 2018, pp. 704–720.
- [34] O. Litany, A. Bronstein, M. Bronstein, and A. Makadia, "Deformable shape completion with graph convolutional autoencoders," in *Proceedings of the IEEE conference on computer vision and pattern recognition*, 2018, pp. 1886–1895.
- [35] L. Antelmi, N. Ayache, P. Robert, and M. Lorenzi, "Sparse multi-channel variational autoencoder for the joint analysis of heterogeneous data," in *International Conference on Machine Learning*. PMLR, 2019, pp. 302–311.
- [36] M. Defferrard, X. Bresson, and P. Vandergheynst, "Convolutional neural networks on graphs with fast localised spectral filtering," *Advances in neural information processing systems*, vol. 29, pp. 3844–3852, 2016.
- [37] M. Garland and P. S. Heckbert, "Surface simplification using quadric error metrics," in *Proceedings of the 24th annual conference on Computer graphics and interactive techniques*, 1997, pp. 209–216.

- [38] N. Wang, Y. Zhang, Z. Li, Y. Fu, W. Liu, and Y.-G. Jiang, “Pixel2mesh: Generating 3d mesh models from single rgb images,” in *Proceedings of the European Conference on Computer Vision (ECCV)*, 2018, pp. 52–67.
- [39] K. He, X. Zhang, S. Ren, and J. Sun, “Deep residual learning for image recognition,” in *Proceedings of the IEEE conference on computer vision and pattern recognition*, 2016, pp. 770–778.
- [40] D. Ulyanov, A. Vedaldi, and V. Lempitsky, “Instance normalisation: The missing ingredient for fast stylisation,” *arXiv preprint arXiv:1607.08022*, 2016.
- [41] L. Trottier, P. Giguere, and B. Chaib-Draa, “Parametric exponential linear unit for deep convolutional neural networks,” in *2017 16th IEEE International Conference on Machine Learning and Applications (ICMLA)*. IEEE, 2017, pp. 207–214.
- [42] A. Nealen, T. Igarashi, O. Sorkine, and M. Alexa, “Laplacian mesh optimisation,” in *Proceedings of the 4th international conference on Computer graphics and interactive techniques in Australasia and South-east Asia*, 2006, pp. 381–389.
- [43] A. Dubrovina, F. Xia, P. Achlioptas, M. Shalah, R. Grosset, and L. J. Guibas, “Composite shape modeling via latent space factorisation,” in *Proceedings of the IEEE/CVF International Conference on Computer Vision*, 2019, pp. 8140–8149.
- [44] O. Ronneberger, P. Fischer, and T. Brox, “U-net: Convolutional networks for biomedical image segmentation,” in *International Conference on Medical image computing and computer-assisted intervention*. Springer, 2015, pp. 234–241.
- [45] C. Sudlow, J. Gallacher, N. Allen, V. Beral, P. Burton, J. Danesh, P. Downey, P. Elliott, J. Green, M. Landray *et al.*, “Uk biobank: an open access resource for identifying the causes of a wide range of complex diseases of middle and old age,” *PLoS medicine*, vol. 12, no. 3, p. e1001779, 2015.
- [46] S. E. Petersen, N. Aung, M. M. Sanghvi, F. Zemrak, K. Fung, J. M. Paiva, J. M. Francis, M. Y. Khanji, E. Lukaschuk, A. M. Lee *et al.*, “Reference ranges for cardiac structure and function using cardiovascular magnetic resonance (cmr) in caucasians from the uk biobank population cohort,” *Journal of Cardiovascular Magnetic Resonance*, vol. 19, no. 1, pp. 1–19, 2017.
- [47] N. Ravikumar, A. Gooya, A. F. Frangi, and Z. A. Taylor, “Generalised coherent point drift for group-wise registration of multi-dimensional point sets,” in *International Conference on Medical Image Computing and Computer-Assisted Intervention*. Springer, 2017, pp. 309–316.
- [48] Y. Xia, X. Chen, N. Ravikumar, C. Kelly, R. Attar, N. Aung, S. Neubauer, S. E. Petersen, and A. F. Frangi, “Automatic 3d+ t four-chamber cmr quantification of the uk biobank: integrating imaging and non-imaging data priors at scale,” *Medical Image Analysis*, p. 102498, 2022.
- [49] A. Paszke, S. Gross, F. Massa, A. Lerer, J. Bradbury, G. Chanan, T. Killeen, Z. Lin, N. Gimelshein, L. Antiga *et al.*, “Pytorch: An imperative style, high-performance deep learning library,” *Advances in neural information processing systems*, vol. 32, pp. 8026–8037, 2019.
- [50] D. P. Kingma and J. Ba, “Adam: A method for stochastic optimisation,” *arXiv preprint arXiv:1412.6980*, 2014.
- [51] Y. Zhou, C. Wu, Z. Li, C. Cao, Y. Ye, J. Saragih, H. Li, and Y. Sheikh, “Fully convolutional mesh autoencoder using efficient spatially varying kernels,” *Advances in Neural Information Processing Systems*, vol. 33, pp. 9251–9262, 2020.
- [52] A. Knapitsch, J. Park, Q.-Y. Zhou, and V. Koltun, “Tanks and temples: Benchmarking large-scale scene reconstruction,” *ACM Transactions on Graphics (ToG)*, vol. 36, no. 4, pp. 1–13, 2017.
- [53] H. Fan, H. Su, and L. J. Guibas, “A point set generation network for 3d object reconstruction from a single image,” in *Proceedings of the IEEE conference on computer vision and pattern recognition*, 2017, pp. 605–613.
- [54] R. H. Davies, C. J. Twining, T. F. Cootes, and C. J. Taylor, “Building 3-d statistical shape models by direct optimisation,” *IEEE Transactions on Medical Imaging*, vol. 29, no. 4, pp. 961–981, 2009.
- [55] B. G. Amidan, T. A. Ferryman, and S. K. Cooley, “Data outlier detection using the chebyshev theorem,” in *2005 IEEE Aerospace Conference*. IEEE, 2005, pp. 3814–3819.